Oxidative Stress Induced by Zero-Valent Iron Nanoparticles and Fe(II) in Human Bronchial Epithelial Cells

CHRISTINA R. KEENAN,[†] REGINE GOTH-GOLDSTEIN,[‡] DONALD LUCAS,[§] AND DAVID L. SEDLAK*,[†]

Department of Civil and Environmental Engineering, University of California at Berkeley, Berkeley, California 94720, Environmental Energy Technologies Division, Lawrence Berkeley National Laboratory, Berkeley, California 94720, and Environmental Health and Safety Division, Lawrence Berkeley National Laboratory, Berkeley, California 94720

Received March 2, 2009. Revised manuscript received April 16, 2009. Accepted April 26, 2009.

To identify the mechanism through which nanoparticulate zero-valent iron (nZVI; $Fe^0_{(s)}$) damages cells, a series of experiments were conducted in which nZVI in phosphate-buffered saline (PBS) was exposed to oxygen in the presence and absence of human bronchial epithelial cells. When nZVI is added to PBS, a burst of oxidants is produced as Fe^0 and ferrous iron (Fe[II]) are converted to ferric iron (Fe[III]). Cytotoxicity and internal reactive oxygen species (ROS) production in cells exposed to nZVI is equivalent to the response observed when cells are exposed to the same concentration of dissolved Fe(II). Experiments conducted in the absence of cells indicate that the oxidant produced during Fe(II) oxidation reacts with methanol and dimethyl sulfoxide, but not with compounds such as *tert*-butanol and benzoate that react exclusively with hydroxyl radical. The role of reactive oxidants produced during Fe(II) oxidation in cytotoxicity and internal ROS production is further supported by experiments in which cell damage was limited by the addition of ligands that prevented Fe(II) oxidation and by the absence of cell damage when the nanoparticles were oxidized prior to exposure. The behavior of the oxidant produced by nZVI is consistent with an oxidant such as the ferryl ion, rather than hydroxyl radical.

Introduction

Zero-valent iron nanoparticles (nZVI) have received significant attention due to their potential applications in environmental remediation. Due to its higher reactivity and potential for delivery deep into the ground, nZVI has the potential to be more effective than granular zerovalent iron for remediation of chlorinated organic solvents, pesticides, and metals (*1, 2*). Several field demonstrations of nZVI have already been documented (*3*) and commercially produced nZVI is available from several sources (*2*). The use of nZVI for groundwater remediation is one of the furthest advanced nanotechnology applications that could result in releases of large quantities of nanoparticles into the environment.

Despite the potential for beneficial applications of nZVI, concerns have been raised about the impact of nanoparticles on human and environmental health (*4*). The small size and high surface area of nanoparticles, combined with their ability to generate reactive oxygen species (ROS) or release toxic metals at cell surfaces, may contribute to the toxicity of nanoparticles (*5*). Oxidative damage is one of the most frequently articulated concerns among scientists studying lung damage induced by particle exposure and the ability of particles to cause oxidative stress has been linked to ROS generation (*6, 7*). Oxidative stress, ROS generation, and inflammation caused by exposure to particulate matter is often correlated with the presence of transition metals, such as iron (*7*−*11*). Iron is believed to cause oxidative stress via redox cycling and ROS generation, resulting in lipid peroxidation and DNA damage (*12, 13*).

Previous investigations of the effect of nZVI on cells have suggested a mechanism in which reduced iron from the nanoparticles is responsible for the observed stress responses. For example, iron nanoparticles were found to cause more damage to rodent microglia and neurons at pH 7 relative to magnetite or nZVI that had been oxidized prior to exposure (*14*). The dose-dependent inactivation of *E. coli* by relatively high concentrations of nZVI at pH 5−5.5 and 8 also was greater than that observed for similar concentrations of nanoparticulate magnetite, maghemite, or oxidized nZVI (*15, 16*). Inactivation was greater in *E. coli* mutants lacking superoxide dismutase, suggesting that ROS also may play a role in inactivation (*15*).

Although the role of reduced iron as a source of ROS has been recognized as a potentially important factor in nZVI toxicity, the underlying chemical mechanisms for the observed toxicity have not been elucidated and previous studies have not fully considered the effect of bioassay test conditions on oxidant production. To assess the mechanism of nZVI toxicity under conditions relevant to nanoparticle inhalation (e.g., during manufacture) and to enable comparison with previous studies of particulate matter toxicity, human bronchial epithelial cells were exposed to nZVI and Fe(II). After exposure, cells were assayed for viability and internal ROS production using previously established techniques and results were compared with results from cell-free experiments using oxidant probe compounds to quantify reactive oxidant production. By manipulating cell assay conditions and by conducting experiments with organic compounds that react selectively with different oxidants, insights were made into mechanisms of cell damage by nZVI and other iron-containing particles.

Materials and Methods

Materials. Details concerning the materials and experimental setup are provided in the Supporting Information (SI). Briefly, phosphate-buffered saline (PBS; 1.06 mM KH_2PO_4, 2.97 mM Na_2HPO_4, 155 mM NaCl) with the pH adjusted to 7.0 with HCl, was used in all experiments, unless indicated. Iron chelators, such as 2,2′-bipyridine (BPY) or desferrioxamine (DFO), or oxidant scavengers, such as dimethyl sulfoxide (DMSO), benzoate (BA), or *tert*-butanol (TBA), were added to PBS in some experiments.

Cell-Free Experiments. Nanoparticulate zero-valent iron was prepared daily as described previously (*2, 17*). Ferrous iron stock solutions were prepared by dissolving ferrous sulfate in 1 mM HNO_3. Weathered nZVI suspensions

* Corresponding author phone: (510) 643-0256; fax: (510) 642-7483; e-mail: sedlak@ce.berkeley.edu.
[†] University of California at Berkeley.
[‡] Environmental Energy Technologies Division.
[§] Environmental Health and Safety Division.

10.1021/es9006383 CCC: $40.75
Published on Web 05/12/2009

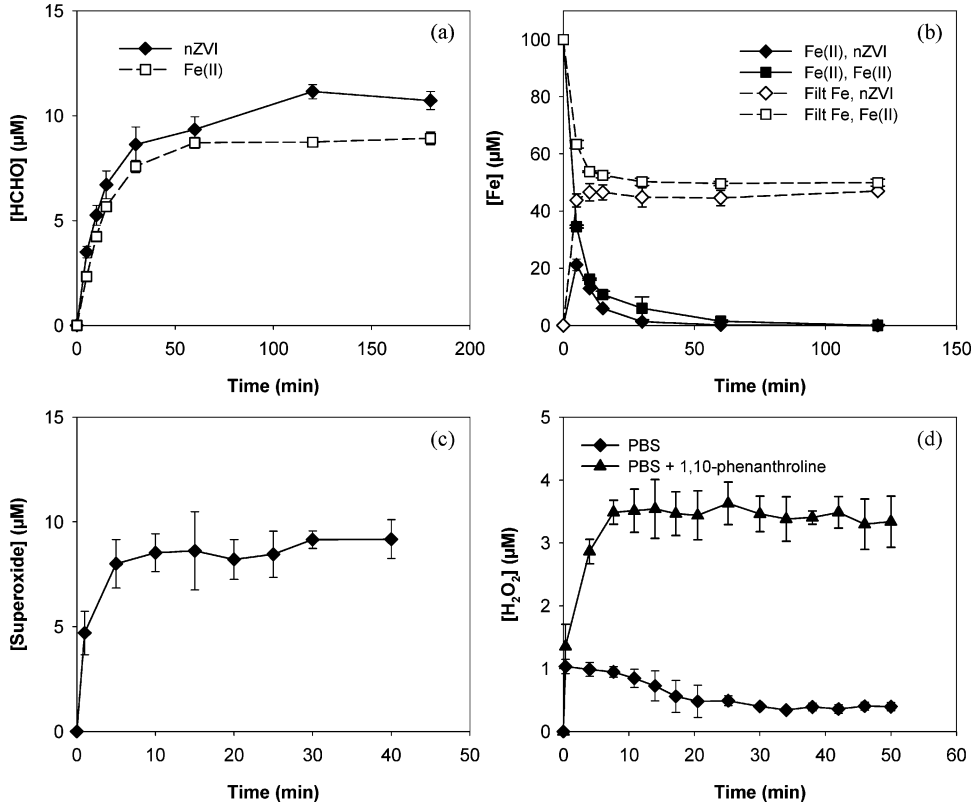

FIGURE 1. (a) Kinetics of HCHO production and (b) filterable Fe(II) and filterable total Fe present after addition of 100 μM nZVI and 100 μM Fe(II) to PBS and 100 mM CH_3OH at pH 7. Production of (c) superoxide and (d) H_2O_2 with and without 1 mM 1,10-phenanthroline by 100 μM nZVI in PBS at pH 7.

were prepared by allowing the diluted nZVI solution to oxidize in air-saturated PBS solutions for 4 h prior to use.

Experiments in the absence of cells were carried out in air-saturated solutions in 60-mL glass serum vials at room temperature (20 ± 2 °C) in the dark. Filterable Fe(II), total filterable iron, and total iron were quantified colorimetrically using ferrozine (*18*), 2,2′-bipyridine (*19*), or desferrioxamine (*20*). Superoxide production was quantified by measuring the colored product of the reaction of XTT reduction by $O_2^{-\cdot}$ (*21, 22*). Hydrogen peroxide was measured using a modified *N,N*-dimethyl phenylendiamine (DPD) method (*18, 23, 24*).

Methanol and benzoate were used as probe compounds to quantify oxidant production and determine the nature of the reactive oxidant. Methanol is oxidized by either $OH^{\cdot}$ or Fe(IV), whereas benzoate reacts with $OH^{\cdot}$ but not Fe(IV) (*25*). The main products from the oxidation of probe compounds, formaldehyde (HCHO) and *para*-hydroxybenzoate, were measured by HPLC as described previously (*25*). Total hydroxybenzoate (HBA) production was estimated using measurements of *para*-hydroxybenzoate.

Equilibrium speciation calculations were performed using MINEQL+, with equilibrium constants added from the NIST Standard Reference Database (*26*) as necessary.

Cytotoxicity Experiments. Human bronchial epithelial cells (cell line 16HBE14o) were seeded into 12- and 24-well plates at a density of 0.5−1 × 10^5 cells per well two days before exposure to nZVI and Fe(II). PBS or PBS containing the appropriate scavenger or iron-chelator were used as controls (SI Table S1). There were at least three wells per condition and Student's *t* test was used to test statistical significance. Cell viability was measured by quantifying lactate dehydrogenase (LDH) released during the one-hour exposure (Sigma Aldrich) and is proportional to membrane damage. The 2′7′-dichlorodihyrdofluorescein diacetate (HD-CF-DA) assay (*27*−*29*) was used to measure ROS production inside the lung cells.

Results

Oxidant Production. The introduction of nZVI or Fe(II) to 100 mM CH_3OH in PBS produced a rapid burst of an oxidant capable of oxidizing methanol to formaldehyde (Figure 1a). Fe(II) released from nZVI or added to PBS was oxidized to Fe(III) within 60 min and Fe(III) slowly precipitated out of solution (Figure 1b). Superoxide and hydrogen peroxide were produced as nZVI was oxidized (Figure 1c−d). Superoxide production by nZVI plateaued at a concentration of ~9 μM after 15 min in the presence of 300 μM XTT. In PBS, nZVI produced 1.0 ± 0.1 μM H_2O_2 after 20 s, which gradually disappeared. The addition of 1,10-phenanthroline to complex Fe(II), and thereby prevent its reaction with H_2O_2 (*30*), allowed H_2O_2 to build up to a concentration of ~3.5 μM after 15 min. Formaldehyde production during oxidation of Fe(II) was slightly lower than that of nZVI due to higher iron solubility in the nZVI system (SI Figure S1).

The choice of solution conditions affected oxidant production by nZVI. Experiments with PBS and Hank's balanced salt solution (HBSS), which has been used in previous nanoparticle toxicity studies (*14, 29*), demonstrated that oxidant production (i.e., HCHO) was approximately three times higher in PBS than it was in HBSS (SI Figure S2). Oxidant production by nZVI in PBS at pH 7 also was 2−3 times higher than it was in 1 mM piperazine-*N,N*′-bis(ethanesulfonic acid) (PIPES), which was used in previous studies because the buffer does not complex iron (*25*), or in 1 mM PIPES with 155 mM NaCl. The addition of bicarbonate to PBS decreased oxidant production, with HCHO production decreasing from 11.2 to 5.6 μM with the addition of 10 mM HCO_3^- (SI Figure S3). Based on this result, lung cells were exposed to nZVI in an incubator with atmospheric levels of CO_2 to minimize the effect of HCO_3^- on Fe(II) speciation and oxidant production. While the presence of 155 mM chloride decreased oxidant production by 29.8 ± 2.7% in 2 mM PIPES, it had a negligible

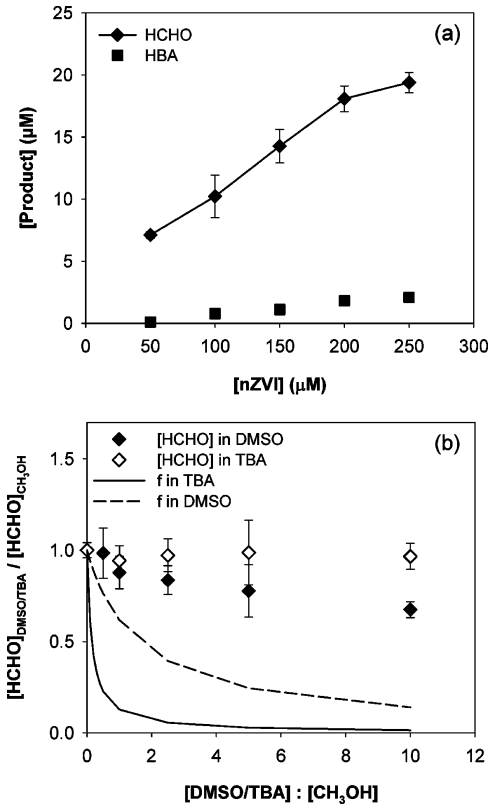

FIGURE 2. (a) HCHO and total HBA production by nZVI in PBS and 100 mM CH_3OH and 5 mM benzoate at pH 7, $t = 60$ min. (b) [HCHO] in DMSO or TBA and methanol/[HCHO] in methanol alone as a function of DMSO and TBA added to 10 mM CH_3OH in PBS at pH 7, for $t = 60$ min. Lines indicate the product formation expected if $OH^{\cdot}$ was the reactive oxidant using published rate constants (*32*).

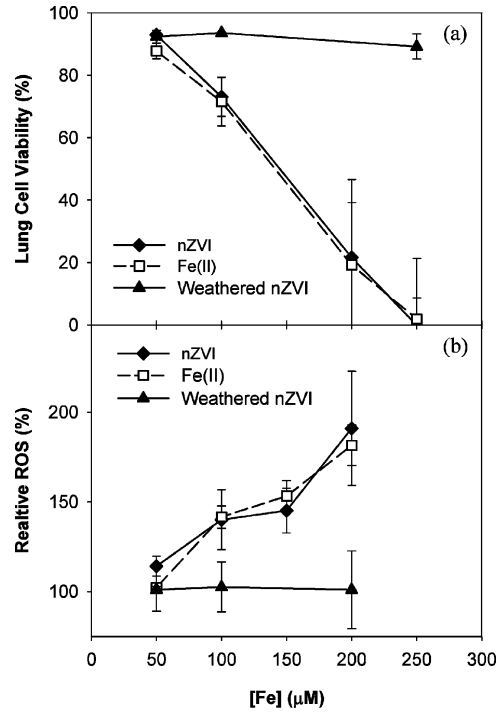

FIGURE 3. (a) Lung cell viability and (b) internal ROS production after a 60 min exposure to nZVI, Fe(II) or weathered nZVI in PBS at pH 7. Data is relative to LDH released by negative controls and lysed cells, and to fluorescence of negative controls, respectively.

impact on oxidation production in the presence of 4 mM phosphate (SI Figure S4). The addition of phosphate to 2 mM PIPES increased both oxidant production and iron solubility (SI Figure S5).

It was necessary to characterize the type of oxidant produced when nZVI and Fe(II) are oxidized at pH 7 in PBS because changes in iron coordination and solubility can change the reactive oxidant from Fe(IV) to $OH^{\cdot}$ (*31*). Under our experimental conditions, the oxidation of nZVI and Fe(II) resulted in more efficient oxidation of methanol than of benzoate (Figure 2a). Competition experiments between DMSO or TBA and CH_3OH demonstrated that at a molar ratio of 10:1, HCHO production decreased by 32.6 ± 4.4% with DMSO and 3.4 ± 7.1% with TBA relative to experiments with methanol alone (Figure 2b). While DMSO decreased methanol oxidation more than TBA, it was less effective than predictions based on published rate constants for reactions of the compounds with $OH^{\cdot}$ (Figure 2b (*32*)).

HCHO production when 200 μM nZVI was exposed to O_2 decreased from 18.1 ± 1.0 μM to 2.5 ± 0.7 μM in the presence of 1 mM BPY, which forms a 3:1 complex with Fe(II) (*26*), and to 7.0 ± 0.6 μM in the presence of 1 mM DFO, which forms 1:1 complexes with both Fe(II) and Fe(III) (Figure 4a (*26*)). According to equilibrium calculations, nearly all Fe(II) exists as $Fe(BPY)_3^{4-}$ in the presence of 1 mM BPY. Equilibrium calculations indicate that Fe^{II}−DFO complexes should account for 46% of total Fe(II) in 1 mM DFO in PBS.

Cytotoxicity. Exposure of human bronchial epithelial cells to nZVI or Fe(II) in PBS resulted in a decrease in viability that followed a dose−response relationship (Figure 3a). After 60 min, 73.1 ± 6% and 21.6 ± 25% of the cells were viable based on the LDH assay when exposed to 100 and 200 μM nZVI, respectively. After exposure to 100 and 200 μM Fe(II), 71.5 ± 8 and 19.1 ± 20% of the cells were viable. Exposing the cells to weathered nZVI resulted in minimal cytotoxicity, with 89.2 ± 3.9% of the cells still viable when exposed to the highest dose of 250 μM. Internal ROS production, as measured with the HDCF-DA assay, followed similar trends (Figure 3b). ROS increased by 370 ± 67%, 357 ± 24%, and 101 ± 22% relative to controls when exposed to 200 μM nZVI, Fe(II), and weathered nZVI, respectively. Control experiments demonstrated that nZVI and Fe(II) could oxidize HDCF, the intermediate compound that is only present inside the cells, to form a fluorescent product, but could not oxidize HDCF-DA directly (SI Figure S6). Weathered nZVI did not oxidize HDCF-DA or HDCF.

The addition of 1 mM DMSO to nZVI solutions resulted in significantly less LDH release compared to cells exposed to nZVI in PBS alone (Figure 4b). The addition of 1 mM TBA or BA to nZVI solutions had a negligible effect on cell viability (SI Table S2). While some variability was observed in response to nZVI among different batches of cells, the difference between LDH released in the presence and absence of DMSO and under all other conditions was statistically significant at both iron doses.

The addition of BPY and DFO (*33*) increased viability and decreased internal ROS production when cells were exposed to nZVI. Viability increased to 79.7 ± 13.7% and 81.6 ± 3.3% when exposed to 200 μM nZVI in the presence of 1 mM BPY or 1 mM DFO, respectively (Figure 4b). Internal ROS production decreased to 168 ± 18% and 156 ± 32% when BPY or DFO were added under the same conditions (Figure 4c).

Discussion

Acute Oxidative Stress. The oxidation of nZVI by oxygen at neutral pH produces a rapid burst of oxidants (Figure 1) according to the following simplified mechanism (*25*):

$$Fe^0_{(s)} + O_2 + 2H^+ \rightarrow Fe(II) + H_2O_2 \qquad (1)$$

$$Fe^0_{(s)} + H_2O_2 + 2H^+ \rightarrow Fe(II) + 2H_2O \quad (2)$$

$$Fe(II) + O_2 \rightarrow Fe(III) + O_2^{-\cdot} \quad (3)$$

$$Fe(II) + O_2^{-\cdot} + 2H^+ \rightarrow Fe(III) + H_2O_2 \quad (4)$$

$$Fe(II) + H_2O_2 \rightarrow oxidant \quad (5)$$

Superoxide and H_2O_2 are produced as intermediates of nZVI and Fe(II) oxidation (reactions 1, 3, 4; Figure 1). The product of the Fenton reaction (reaction 5) is capable of oxidizing organic compounds and may be $OH^{\cdot}$ or Fe(IV). As described below, Fe(IV), or another oxidant that exhibits reactivity different from that of $OH^{\cdot}$, is the main oxidant produced in reaction 5 under conditions used in the bioassay. According to reactions 1−5, at least 33.3 μM of oxidant should have been produced via reaction 5 as 100 μM of nZVI was converted to Fe(III). However, reactive oxidant production at circumneutral pH is typically lower than the theoretical maximum due to iron precipitation, which presumably results in consumption of oxidants through surface reactions (*25*). Assuming that methanol and XTT react only with oxidants that are not consumed in surface reactions, the data in Figure 1a and c indicate that approximately 9 μM of $O_2^{-\cdot}$ is produced during the first 10 min of the reaction and that all of it is converted into an oxidant in reaction 5 (i.e., reactions 3−5).

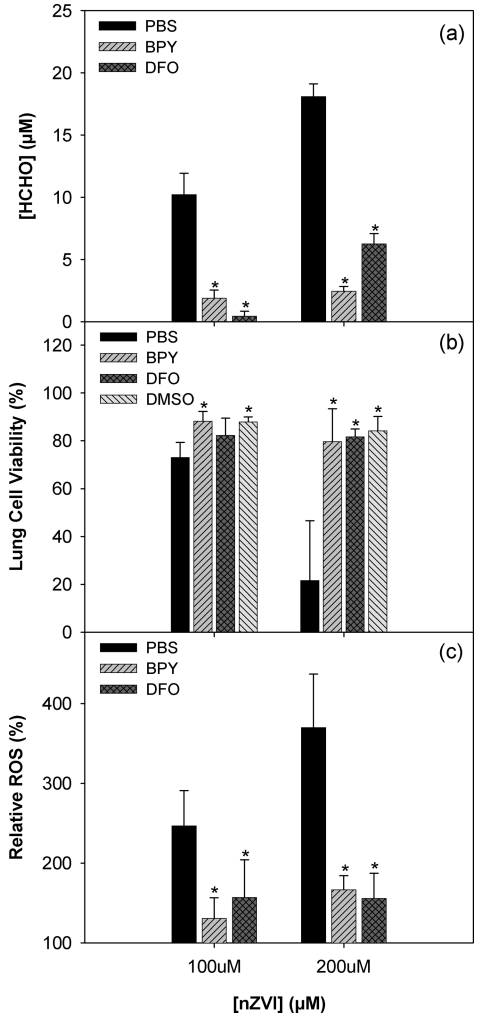

FIGURE 4. (a) HCHO production in 100 mM CH_3OH, (b) lung cell viability, and (c) internal ROS production by 100−200 μM nZVI in PBS, 1 mM 2,2′-bipyridine (BPY) in PBS, 1 mM desferrioxamine B (DFO), or 1 mM DMSO in PBS at pH 7, t = 60 min. The asterisk indicates that the data is statistically significant compared to the response in PBS.

Superoxide production is approximately equivalent to HCHO production (reactions 4−5). The concentration of H_2O_2 that accumulated in the presence of 1,10-phenanthroline (Figure 1d) is less than half of the concentration of superoxide and HCHO because 1,10-phenanthroline slows Fe(II) oxidation by O_2 and H_2O_2, and H_2O_2 is only produced by reaction 1 when 1,10-phenanthroline is present. The presence of 1,10-phenanthroline limits the formation of passivation layers on the nanoparticle surface, potentially allowing more H_2O_2 produced by reaction 1 to reach the bulk solution, as observed previously with EDTA (*31*). In the absence of 1,10-phenathroline, H_2O_2 produced by reaction 4 disappears rapidly through reaction 5 and the measured H_2O_2 concentration is not indicative of the total amount of H_2O_2 produced.

Previous studies demonstrated that Fe(II) oxidation via reactions 3−5 is the dominant mechanism for oxidant production at circumneutral pH, with nZVI serving as source of Fe(II) (*25*). The role of Fe(II) in oxidant production under conditions used in the bioassay was confirmed; the addition of nZVI or Fe(II) to PBS resulted in the formation of nearly identical concentrations of formaldehyde (Figures 1, S1). Between 5 and 10% more filterable iron was present after an hour when nZVI was added and this resulted in slightly higher HCHO production as Fe(II) was converted to Fe(III) (SI Figure S1).

Results from the bioassays indicate that the presence of Fe(II) is a prerequisite for cell damage and that $Fe^0_{(s)}$ in the nanoparticles is not directly responsible for cell damage. Viability and internal ROS production by human bronchial epithelial cells exposed to nZVI for 60 min followed a dose−response relationship (Figure 3). For both oxidative stress assays, the response of the cells to dissolved Fe(II) was equivalent to that of nZVI. Exposure to nZVI that had been allowed to oxidize in PBS for 4 h did not cause a significant response, in agreement with previous studies with nanoparticulate magnetite, nanoparticulate maghemite, and aged nZVI (*14, 15*). These observations suggest that acute cytotoxicity is due to the rapid burst of oxidants produced during Fe(II) oxidation and that the aged nanoparticles consisting of Fe(III) oxides are much less toxic than fresh nZVI. While Fe(III)-containing oxides did not cause strong responses in cell cultures during the 60 min exposure, it is possible that reductants produced by cells, such as glutathione or superoxide, can reduce Fe(III) to Fe(II) (*34*), leading to cell damage over longer time periods.

The role of Fe(II) in oxidant production was further supported by experiments conducted in the presence of iron chelators. The addition of BPY and DFO decreased HCHO production by nZVI (Figure 4a). BPY decreases oxidant production by slowing the rate of Fe(II) oxidation by O_2 and H_2O_2 (*23*). Therefore, oxidant production is limited in the presence of BPY because Fe(II) was not completely oxidized during the 60 min experiment. The ability of BPY to lower HCHO production indicates that the reaction of Fe(II) with O_2 and H_2O_2 (reactions 3−5) is necessary for oxidant production. DFO forms very strong complexes with Fe(III) ($K^{conditional}_{Fe(III)-HL} = 10^{30.6}$ (*26*)) relative to Fe(II) ($K^{conditional}_{Fe(II)-H_2L} = 10^{7.2}$ (*26*)) and, as a result, the rate of Fe(II) oxidation by O_2 is significantly accelerated in the presence of excess DFO at pH 7 (*35*). The addition of DFO to our system resulted in a significant decrease in HCHO production (Figure 4a). While it is possible that DFO can scavenge radicals (*36*), it is unlikely that DFO served as the main oxidant sink in the cell-free experiments because the concentration of the probe compound, methanol, was 2 orders of magnitude higher than that of DFO. Furthermore, oxidation of Fe(II)-DFO by O_2 does not produce an oxidant capable of oxidizing terephthalate or ethanol (*35*). Therefore, the decrease in HCHO production by nZVI in the presence of DFO is most likely is attributable to the fast oxidation of Fe(II) and decreased

production of oxidants capable of oxidizing probe compounds when DFO-complexed Fe(II) is oxidized.

The effects of iron-chelating ligands on nZVI toxicity to the epithelial cells supports our hypothesis about the role of Fe(II) in the bioassay response. The ability of BPY and DFO to limit LDH release upon exposure to nZVI suggests that cytotoxicity is due to the formation of oxidants during Fe(II) oxidation (Figure 4b). Addition of BPY decreases the rate of oxidation of Fe(II) by O_2 (reaction 3), which minimizes oxidative damage. DFO results in rapid oxidation of Fe(II) with limited oxidant production and formation of a hexadentate complex with Fe(III) (*20*) that cannot be reduced by superoxide to Fe(II) at a significant rate (*36*), thereby preventing iron redox cycling.

Under the conditions of the bioassay, Fe(II) oxidation happens quickly (Figure 1b) and it is unlikely that significant quantities of added Fe(II) were taken up by the cells during the 60 min experiment. Therefore, internal ROS production, as measured with the HDCF-DA assay, most likely was triggered by external oxidative stress. Oxidative stress activates redox-responsive signaling pathways in cells, including the expression of genes that play a role in responses to inflammation and result in intracellular ROS production (*37*). The ability of BPY and DFO to limit internal ROS production in cells exposed to nZVI (Figure 4c) is additional evidence that Fe(II) oxidation at the membrane surface is involved in the bioassay response.

Effect of Phosphate, Chloride, And Bicarbonate on Oxidant Yield. Previous studies on nZVI indicate that the release and subsequent oxidation of Fe(II) by O_2 is the dominant mechanism of oxidant production at neutral pH values (*25*). Ligands that accelerate the rate of Fe(II) oxidation or increase iron solubility were found to enhance oxidant production, with yields approaching theoretical maxima in some cases (*31*). Because the bronchial epithelial cells can not tolerate PIPES, phosphate and bicarbonate buffers are often used in bioassays. Solution conditions used for exposures can affect oxidant production in reaction 5 through changes in iron coordination. In our system, oxidant production was approximately 2−3 times higher in PBS than PIPES, saline-PIPES, or HBSS (SI Figure S2). These findings can be explained by considering the effect of the ligands on Fe(II) oxidation rates and on iron solubility and are described in detail in the Supporting Information. Although it is difficult to directly compare these results to conditions in lungs because epithelial lining fluid contains iron transport proteins (*38*) and antioxidants, such as ascorbic acid and glutathione (*39*), PBS is more likely to be more representative of conditions encountered in vivo than HBSS with respect to bicarbonate. The bicarbonate concentration in HBSS (i.e., >4 mM) is higher than the concentration encountered in air-saturated solutions and lowers oxidant production through Fe(II) precipitation.

Role of Fe(IV) in Cell Damage. Although the hydroxyl radical is often cited as the main product of the Fenton reaction, an alternate oxidant, such as the ferryl ion, may be formed under some conditions (*40*). For example, Fe(IV) appears to be the primary oxidant produced by ZVI at circumneutral pH values in the absence of ligands (*23, 25*) and by Fe(II) in phosphate-buffered solutions (*41*). In our experimental system, the oxidation of nZVI and Fe(II) by O_2 produced an oxidant capable of oxidizing methanol more efficiently than benzoate in PBS at pH 7 (Figure 2a). These results are similar to previous observations made in the nZVI system in the absence of ligands and are consistent with production of Fe(IV) or an oxidant other than $OH^{\cdot}$. Furthermore, addition of DMSO or TBA had a much smaller effect on methanol oxidation than expected from predictions made with measured rate constants for the reaction of $OH^{\cdot}$ with DMSO, TBA, and CH_3OH (Figure 2b). The inability of TBA or DMSO to prevent methanol oxidation is inconsistent with the presence of $OH^{\cdot}$ and provides further evidence for an alternate oxidant, such as Fe(IV), in this system. In addition, the observation that DMSO scavenges the oxidant more effectively than TBA indicates that DMSO is more reactive with the oxidant than TBA.

Bioassays performed in the presence of DMSO, TBA, and benzoate suggest that the oxidant responsible for methanol oxidation also plays an important role in epithelial cell damage. Among these radical scavengers, only DMSO was able to limit cytotoxicity in cells exposed to nZVI (Figure 4b; SI Table S2), which is consistent with damage from Fe(IV) production during Fe(II) oxidation.

Implications for Nanoparticle and Particulate Matter Toxicity. In agreement with earlier studies with Fe(III)-containing nanoparticles (*14, 15*), we found that aged nZVI, which consists mainly of Fe(III)-(hydr)oxides, had a minimal effect on cells because reactive oxidants were not produced (reactions 3-5) in the absence of Fe(II). Fe(III) can be reduced in vivo (*13, 34, 38*) and the presence of Fe(III) in particles can lead to oxidative damage over longer time periods. The presence of transition metals, such as iron, in particulate matter (*7*−*10, 37*) and silicates (*29, 42*) is positively correlated with toxicity. Often the soluble portions of particulate matter caused the same toxicity as the particles (e.g., *8, 9*), suggesting that the toxic effect was due to the metals released into solution rather than the particles themselves.

In this study we demonstrated that the presence of Fe(II) in particles results in the production of a burst of oxidants that may cause lung irritation. Previous researchers have provided ample evidence that oxidants produced as iron undergoes redox reactions cause oxidative stress (*12, 13*), and our observation that nZVI toxicity to bronchial epithelial cells is related to the release and subsequent oxidation of Fe(II) illustrates the crucial role of iron oxidation state in the initial stress response. Although Fe(III) is the thermodynamically favored form of iron in the presence of O_2, aerosol particles, fog, and cloudwater can contain considerable amounts of Fe(II), especially under acidic conditions (*43, 44*). Upon inhalation, the increase in pH that occurs when acidic aerosols encounter the well-buffered lung fluid will result in the rapid oxidation of Fe(II) and a burst of oxidants, as observed with the ZVI nanoparticles. Therefore, the oxidation state of Fe in ambient or engineered particles may be an important factor to consider in evaluations of particle toxicity.

Acknowledgments

This research was supported by the U.S. National Institute of Environmental Health Sciences (Grant P42 ES04705) and the U.S. Department of Energy (Contract No. DE-AC02-05CH11231). The human bronchial epithelial cell line 16HBE14o used for the exposure experiments was provided by Dieter Gruenert at California Pacific Medical Center Research Institute. We thank Kath Ratcliff and Ken Dong for providing access to the fluorescence microplate reader, Marion Russell and Amara Holder for their support at LBNL, and Martyn Smith and Kara Nelson for their comments and advice.

Supporting Information Available

Detailed methodology, discussion of the effect of ligands, Figures S1−S7, and Tables S1−S2. This material is available free of charge via the Internet at http://pubs.acs.org.

Literature Cited

(1) Zhang, W. Nanoscale iron particles for environmental remediation: An overview. *J. Nanopart. Res.* **2003**, *5*, 323–332.
(2) Nurmi, J. T.; Tratnyek, P. G.; Sarathy, V.; Baer, D. R.; Amonette, J. E.; Pecher, K.; Wang, C. M.; Linehan, J. C.; Matson, D. W.;

Penn, R. L.; Driessen, M. D. Characterization and properties of metallic iron nanoparticles: Spectroscopy, electrochemistry, and kinetics. *Environ. Sci. Technol.* **2005**, *39*, 1221–1230.
(3) Li, L.; Fan, M.; Brown, R. C.; Van Leeuwen, J.; Wang, J.; Wang, W.; Song, Y.; Zhang, P. Synthesis, properties, and environmental applications of nanoscale iron-based materials: A review. *Crit. Rev. Environ. Sci. Technol.* **2006**, *36*, 405–431.
(4) *Nanoscience and Nanotechnologies: Opportunities and Uncertainties*; The Royal Society and The Royal Academey of Engineering: London, 2004.
(5) Nel, A.; Xia, T.; Madler, L.; Li, N. Toxic potential of materials at the nanolevel. *Science* **2006**, *311*, 622–627.
(6) Xia, T.; Kovochich, M.; Brant, J.; Hotze, M.; Sempf, J.; Oberley, T.; Sioutas, C.; Yeh, J.; Wiesner, M.; Nel, A. Comparison of the abilities of ambient and manufactured nanoparticles to induce cellular toxicity according to an oxidative stress paradigm. *NanoLetters* **2006**, *6*, 1794–1807.
(7) Frampton, M. W.; Ghio, A. J.; Samet, J. M.; Carson, J. L. Effects of aqueous extracts of PM_{10} filters from the Utah Valley on human airway epithelial cells. *Am. J. Physiol. Lung Cell Mol. Physiol.* **1999**, *277*, 960–967.
(8) Jiménez, L. A.; Thompson, J.; Brown, D. A.; Rahman, I. Activation of NF-κB by PM_{10} occurs via an iron-mediated mechanism in the absence of IκB degradation. *Toxicol. Appl. Pharmacol.* **2000**, *166*, 101–110.
(9) Donaldson, K.; Brown, D. A.; Mitchell, C.; Dineva, M. Free radical activity of PM_{10}: Iron-mediated generation of hydroxyl radicals. *Environ. Health Perspect.* **1997**, *105*, 1285–1289.
(10) Zhang, Y.; Schauer, J. J.; Shafer, M. M.; Hannigan, M. P.; Dutton, S. J. Source apportionment of in vitro reactive oxygen species bioassay activity from atmospheric particulate matter. *Environ. Sci. Technol.* **2008**, *42*, 7502–7509.
(11) Vidrio, E.; Phuah, C. H.; Dillner, A. M.; Anastasio, C. Generation of hydroxyl radicals from ambient fine particles in a surrogate lung fluid solution. *Environ. Sci. Technol.* **2009**, *43*, 922–927.
(12) Stohs, S. J.; Bagchi, D. Oxidative mechanisms in the toxicity of metal ions. *Free Radical Biol. Med.* **1995**, *18*, 321–336.
(13) Valko, M.; Morris, H.; Cronin, M. T. D. Metals, toxicity and oxidative stress. *Curr. Med. Chem.* **2005**, *12*, 1161–1208.
(14) Phenrat, T.; Long, T. C.; Lowry, G. V.; Veronesi, B. Partial oxidation ("aging") and surface modification decrease the toxicity of nanosized zerovalent iron. *Environ. Sci. Technol.* **2009**, *43*, 195–200.
(15) Auffan, M.; Achouak, W.; Rose, J. B.; Roncato, M.; Cheneac, C.; Waite, D. T.; Masion, A.; Woicik, J.; Wiesner, M. R.; Bottero, J. Relation between the redox state of iron-based nanoparticles and their cytotoxicity toward *Escherichia coli*. *Environ. Sci. Technol.* **2008**, *42*, 6730–6735.
(16) Lee, C.; Kim, J. Y.; Lee, W. I.; Nelson, K. L.; Yoon, J.; Sedlak, D. L. Bactericidal effect of zero-valent iron nanoparticles on Escherichia coli. *Environ. Sci. Technol.* **2008**, *42*, 4927–4933.
(17) Wang, C. B.; Zhang, W. Synthesizing nanoscale iron particles for rapid and complete dechlorination of TCE and PCBs. *Environ. Sci. Technol.* **1997**, *31*, 2154–2156.
(18) Voelker, B. M.; Sulzberger, B. Effects of fulvic acid on Fe(II) oxidation by hydrogen peroxide. *Environ. Sci. Technol.* **1996**, *30*, 1106–1114.
(19) Nguyen, T. H.; Shannon, P. J.; Hoggard, P. E. Kinetics of the photooxidation of tris(bipyridine)iron(II) in chloroform. *Inorg. Chim. Acta* **1999**, *291*, 136–141.
(20) Monzyk, B.; Crumbliss, A. Kinetics and mechanism of the stepwise dissociation of iron(III) from ferrioxamine B in aqueous acid. *J. Am. Chem. Soc.* **1982**, *104*, 4921–4929.
(21) Hotze, E. M.; Labille, J.; Alvarez, P.; Wiesner, M. R. Mechanisms of photochemistry and reactive oxygen production by fullerene suspensions in water. *Environ. Sci. Technol.* **2008**, *42*, 4175–4180.
(22) Sutherland, M. W.; Learmonth, B. A. The tetrazolium dyes MTS and XTT provide new quantitative assays for superoxide and superoxide dismutase. *Free Radical Res.* **1997**, *27*, 283–289.
(23) Katsoyiannis, I. A.; Ruettimann, T.; Hug, S. J. pH dependence of Fenton reagent generation and As(III) oxidation and removal by corrosion of zero valent iron in aerated water. *Environ. Sci. Technol.* **2008**, *42*, 7424–7430.
(24) Bader, H.; Sturzenegger, V.; Hoigne, J.; Photometric method for the determination of low concentrations of hydrogen peroxide by the peroxidase catalyzed oxidation of, N. N-diethyl-p-phenylenediamine (DPD). *Water Res.* **1988**, *22*, 1109–1115.
(25) Keenan, C. R.; Sedlak, D. L. Factors affecting the yield of oxidants from the reaction of nanoparticulate zero-valent iron and oxygen. *Environ. Sci. Technol.* **2008**, *42*, 1262–1267.
(26) *NIST Critically Selected Stability Constants of Metal Complexes Database, Version 8.0*; Smith, R. M.; Martell, A. E., Eds.; National Institute of Standards and Technology: Gaithersburg, MD, 2004.
(27) Halliwell, B.; Whiteman, M. Measuring reactive species and oxidative damage in vivo and in cell culture: How should you do it and what do the results mean? *Br. J. Pharmacol.* **2004**, *142*, 231–255.
(28) Jakubowski, W.; Bartosz, G. 2,7-Dichlorofluorescin oxidation and reactive oxygen species: What does it measure. *Cell Biol. Int.* **2000**, *24*, 757–760.
(29) Limbach, L. K.; Wick, P.; Manser, P.; Grass, R. N.; Bruinink, A.; Stark, W. J. Exposure of engineered nanoparticles to human lung epithelial cells: Influence of chemical composition and catalytic activity on oxidative stress. *Environ. Sci. Technol.* **2007**, *41*, 4158–4163.
(30) Duesterberg, C. K.; Cooper, W. J.; Waite, T. D. Fenton-mediated oxidation in the presence and absence of oxygen. *Environ. Sci. Technol.* **2005**, *39*, 5052–5058.
(31) Keenan, C. R.; Sedlak, D. L. Ligand-enhanced reactive oxidant generation by nanoparticulate zero-valent iron and oxygen. *Environ. Sci. Technol.* **2008**, *42*, 6936–6941.
(32) Buxton, G. V.; Greenstock, C. L.; Helman, W. P.; Ross, A. B. Critical review of rate constants for reactions of hydrated electrons, hydrogen atoms and hydroxyl radicals in aqueous solution. *J. Phys. Chem. Ref. Data* **1988**, *17*, 513–886.
(33) Kicic, A.; Chua, A. C. G.; Baker, E. Effect of iron chelators on proliferation and iron uptake in hepatoma cells. *Cancer* **2001**, *92*, 3093–3110.
(34) Donaldson, K.; Tran, C. L. Inflammation caused by particles and fibers. *Inhal. Toxicol.* **2002**, *14*, 5–27.
(35) Welch, K. D.; Davis, T. Z.; Aust, S. D. Iron autoxidation and free radical generation: Effects of buffers, ligands, and chelators. *Arch. Biochem. Biophys.* **2002**, *397*, 360–369.
(36) Halliwell, B. Protection against tissue damage in vivo by desferrioxamine: What is its mechanism of action. *Free Radical Biol. Med.* **1989**, *7*, 645–651.
(37) Donaldson, K.; Stone, V.; Borm, P. J. A.; Jimenez, L. A. Oxidative stress and calcium signaling in the adverse effects of environmental particles (PM_{10}). *Free Radical Biol. Med.* **2003**, *34*, 1369–1382.
(38) Turi, J. L.; Yang, F.; Garrick, M. D.; Piantadosi, C. A. The iron cycle and oxidative stress in the lung. *Free Radical Bio. Med.* **2004**.
(39) Sun, G.; Crissman, K.; Norwood, J.; Richards, J.; Slade, R.; Hatch, G. E. Oxidative interactions of synthetic lung epithelial lining fluid with metal-containing particulate matter. *Am. J. Physiol. Lung Cell. Mol. Physiol.* **2001**, *281*, 807–815.
(40) Goldstein, S.; Meyerstein, D.; Czapski, G. The Fenton reagents. *Free Radical Biol. Med.* **1993**, *15*, 435–445.
(41) Reinke, L. A.; Rau, J. M.; McCay, P. B. Characteristics of an oxidant formed during iron(II) autoxidation. *Free Radical Biol. Med.* **1994**, *16*, 485–492.
(42) Ghio, A. J.; Kennedy, T. P.; Whorton, A. R.; Crumbliss, A. L. Role of surface complexed iron in oxidant generation and lung inflammation induced by silicates. *Am. J. Physiol.* **1992**, *263*, L511–L518.
(43) Majestic, B. J.; Schauer, J. J.; Shafer, M. M. Application of synchrotron radiation for measurement of iron red-ox speciation in atmospherically processed aerosols. *Atmos. Chem. Phys.* **2007**, *7*, 2475–2487.
(44) Sedlak, D. L.; Hoigné, J.; David, M. M.; Colvile, R. N.; Seyffer, E.; Acker, K.; Wiepercht, W.; Lind, J. A.; Fuzzi, S. The cloudwater chemistry of iron and copper at Great Dun Fell, UK. *Atmos. Environ.* **1997**, *31*, 2515–2526.

ES9006383